

# Strengthening of Ti–6Al–4V Alloy by Short-Time Duplex Heat Treatment

Tatsuro Morita<sup>1</sup>, Kei Hatsuoka<sup>2</sup>, Takashi Iizuka<sup>1</sup> and Kazuhiro Kawasaki<sup>3</sup>

<sup>1</sup>Department of Mechanical & System Engineering, Kyoto Institute of Technology, Kyoto 606-8585, Japan

<sup>2</sup>Automotive Systems Company, Matsushita Electric Industrial Co., Ltd., Yokohama 224-8539, Japan

<sup>3</sup>Technical Department, Neturen Co., Ltd., Kanagawa 254-0013, Japan

The effect of short-time duplex heat treatment on the microstructure and mechanical properties of Ti–6Al–4V alloy was investigated. This heat treatment consisted of solution treatment at 1203 K for 60 s and subsequent water-quenching plus aging at 753, 853 and 953 K for 40 s. The yield strength and tensile strength of the alloy were significantly increased by the above heat treatment and their maximum improvement rates reached about 25%. It was thought that this strengthening was caused by the formation of  $\alpha'$  martensite phase with quenching after the short-time solution treatment and the precipitation of fine  $\alpha$  phase in the retained  $\beta$  phase during the short-time aging. In spite of the remarkable improvement in the strength, the ductility of the heat-treated materials remained above the level of the non-treated material, most likely because strain-induced martensite transformation occurred in  $\beta$  phase which was retained even after the short-time aging.

(Received February 16, 2005; Accepted May 23, 2005; Published July 15, 2005)

**Keywords:** titanium-6 aluminum-4 vanadium alloy, duplex heat treatment, short time, microstructure,  $\alpha'$  martensite phase, retained  $\beta$  phase, strain-induced transformation, hardness, mechanical properties

## 1. Introduction

Ti–6Al–4V alloy has been widely used for lightweight parts and members in a variety of industrial products since its first production in 1954. At the present time, this typical  $\alpha + \beta$  alloy covers 56% of the titanium market in the USA.<sup>1)</sup> The widespread application of Ti–6Al–4V alloy results from its light weight, good corrosion resistance and excellent combination of static strength and ductility. Moreover, this alloy has a potential for further strengthening through tailoring microstructures. Owing to this attractive potential, many studies have investigated for heat treatments to obtain various microstructures and their effect on the mechanical properties of the alloy.<sup>2–18)</sup>

One of the well-known heat treatments is solution treatment and quenching plus aging. With this series of heat treatment, the tensile strength of Ti–6Al–4V alloy is increased by the transformation of  $\beta$  phase to  $\alpha'$  martensite phase and its decomposition to fine  $\alpha$  and  $\beta$  phases.<sup>2–8)</sup> However, the above heat treatment has a problem that it takes a long time. On the other hand, several authors have reported that the tensile strength of the alloy is improved without a reduction in ductility by only solution treatment at 1173 K and quenching.<sup>9,10)</sup> For the quenched material, they have pointed out that the mechanical properties are closely related to strain-induced martensite transformation of retained  $\beta$  phase under an applied stress as well as the formation of  $\alpha'$  phase.

Recently, the authors showed that Ti–6Al–4V alloy can be strengthened by short-time induction heating at over 1173 K for 60 s and quenching.<sup>17)</sup> We thus further investigated the effect of short-time duplex heat treatment, consisting of solution treatment at 1243 K for 60 s and quenching plus aging at 773 K for 40 s, on the mechanical properties of the alloy. As a result, while the tensile strength was remarkably increased from 1110 to 1450 MPa, the reduction of area was decreased from 36 to 17%.<sup>18)</sup> This result suggested that significant strengthening of Ti–6Al–4V is possible with the duplex heat treatment. However, as the alloy is originally

well-balanced in terms of strength and ductility, deterioration of ductility would be undesirable.

To maintain the ductility, we paid attention to the strain-induced transformation of the retained  $\beta$  phase mentioned above.<sup>9,10)</sup> If the short-time solution treatment is conducted at a temperature slightly lower than that used in the previous study, a larger amount of  $\beta$  phase can be retained with the formation of  $\alpha'$  phase by quenching. Then, if the amount of retained  $\beta$  phase is controlled by reheating, it is possible to obtain a well-balanced microstructure which includes both hard  $\alpha'$  phase and an appropriate amount of retained  $\beta$  phase. In such a microstructure, while the  $\alpha'$  phase contributes to the strengthening, the retained  $\beta$  phase can play an effective role in maintaining the ductility through the strain-induced transformation.

From the above viewpoint, Ti–6Al–4V alloy was solution-treated at 1203 K for 60 s and was water-quenched, and then it was aged at temperatures between 753–953 K for 40 s. For the heat-treated materials, we carried out detailed metallographic examinations including the observations of microstructures, X-ray diffraction and selected area electron diffraction measurements as well as the hardness measurements and tensile tests. Through those experiments, we investigated the effect of the above short-time duplex heat treatments on the microstructure and mechanical properties of Ti–6Al–4V alloy.

## 2. Materials and Experimental Methods

The starting material was mill-annealed Ti–6Al–4V rods of 14 mm diameter. The chemical composition is shown in Table 1. Before the main tests described below, the specimens with the configuration shown in Fig. 1(a) were prepared to obtain aging curves for a wide range of aging

Table 1 Chemical compositions (mass%).

Al	V	C	N	O	Fe	H	Ti
6.37	4.11	0.01	0.01	0.10	0.13	0.0009	Bal.

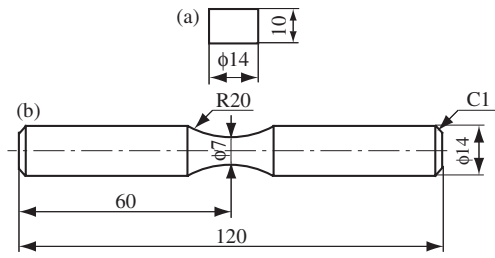


Fig. 1 Configurations of the specimens for: (a) the observations of optical microstructures, X-ray diffraction measurements and hardness measurements; (b) tensile tests (mm).

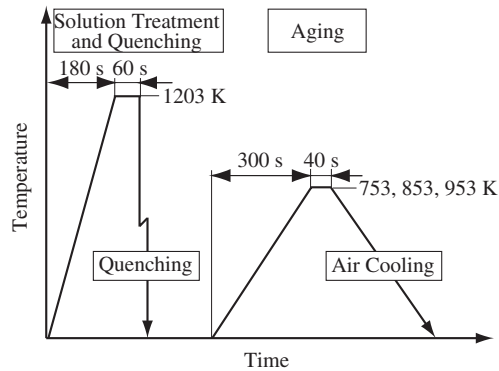


Fig. 2 Conditions of heat treatments.

conditions. The specimens were solution-treated at 1203 K for 60 s in air and water-quenched, and aged at 753–953 K for 40 s–16.2 ks. After the heat treatments, the test sections were mechanically polished with emery papers (100–2000 mesh) and alumina powders (diameter: 0.03  $\mu\text{m}$ ). The surface oxide layer formed during the heat treatments was completely removed by the polishing. For all the materials, measurements of conventional microvickers hardness were made under a load of 2.94 N.

In the main tests, the alloy rods were machined to the specimen configurations shown in Figs. 1(a) and (b). Then, the specimens were heat-treated in air under the conditions shown in Fig. 2. Hereafter, the solution treatment and quenching is designated “STQ treatment” and the duplex heat treatment consisting of the STQ treatment and aging are called “STA treatment”. After the heat treating, the test sections were polished using the method described above.

Optical metallography was made on the specimens etched by Kroll’s reagent. The microvickers hardness of  $\alpha$  phase and prior  $\beta$  phase were measured under a load of 19.6 mN using a super-microvickers tester. For transmission electron microscopy (TEM), we prepared thin discs of 3 mm diameter. The discs were carved from the heat-treated materials and were carefully polished with alumina powders. Thinning of the observation region was conducted by ion-milling. Electron diffraction patterns were obtained at the same positions where the observations of microstructures were carried out. X-ray diffraction measurements were made using the angle  $2\theta$  from  $33^\circ$  to  $43^\circ$  by  $0.02^\circ$  (X-ray: Cu  $K\alpha$ ). The tensile testing was conducted at the displacement ratio of 5.0  $\mu\text{m}/\text{s}$  and then the fracture surface was observed with a scanning electron microscope.

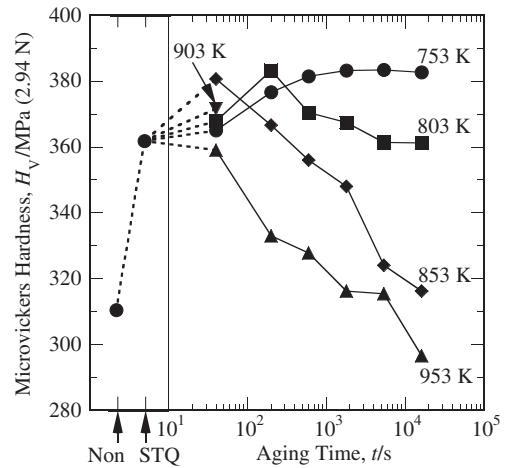


Fig. 3 Aging curves.

### 3. Experimental Results and Discussions

#### 3.1 Hardness and microstructures

Figure 3 shows the change in hardness with the STQ treatment and aging for a wide range of conditions. As shown in the figure, hardness was significantly increased only by the STQ treatment. It is thought that this increase of hardness was mainly due to the formation of  $\alpha'$  phase by quenching. With the subsequent aging for a short time (40 s), hardness was further increased more than the value at the STQ condition except for the aging at 953 K. The time needed to reach the maximum hardness was shortened by elevating the aging temperature and the reduction in hardness began earlier. Especially, in case of the aging at 953 K, hardness continuously decreased from 40 s without any increase in hardness. Such acceleration of aging with the elevation of temperature probably resulted from the fast decomposition of the  $\alpha'$  phase.

In the above results, it is noteworthy that the hardness of the material aged at 853 K for 40 s was about at that obtained by aging at 753 and 803 K for a longer time. This result suggests that the aging at 853 K can remarkably improve the strength of the alloy in a short time. Hereafter, we focused on the effect of aging for 40 s.

Firstly, the microstructures of the non-treated, STQ-treated and STA-treated materials were optically observed. The results are given in Fig. 4. In the non-treated material (Fig. 4(a)), a lot of small dark points show  $\beta$  phase and the other bright region corresponds to  $\alpha$  phase. As can be seen from Fig. 4(b), prior  $\beta$  phase grew greatly with the STQ treatment even for 60 s. However, if the material at the STQ condition was further aged at 753–953 K for 40 s, no remarkable change in the microstructure occurred (Figs. 4(c)–(e)).

In the materials aged for 40 s, although no significant difference in the microstructure was optically observed, hardness was clearly different depending on the aging temperature (Fig. 3). To clarify the phase which contributed to the hardening, hardness measurements of  $\alpha$  phase and  $\beta$  phase were conducted under a very low load (19.6 mN). The results are shown in Fig. 5 with the average hardness data measured under the higher load shown in Fig. 3. As can be

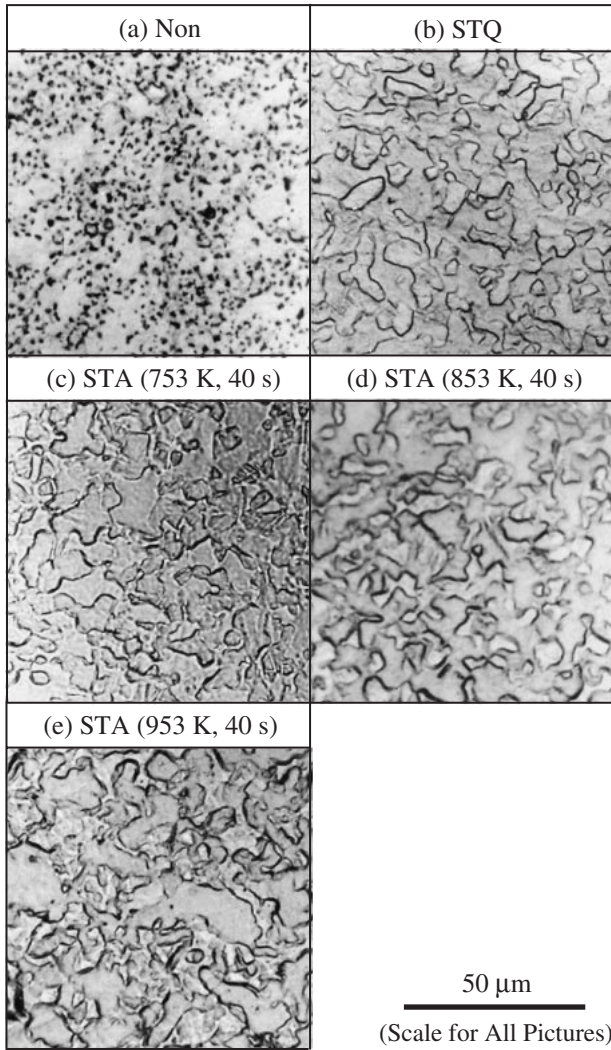


Fig. 4 Microstructures optically observed (the aging conditions are shown in brackets).

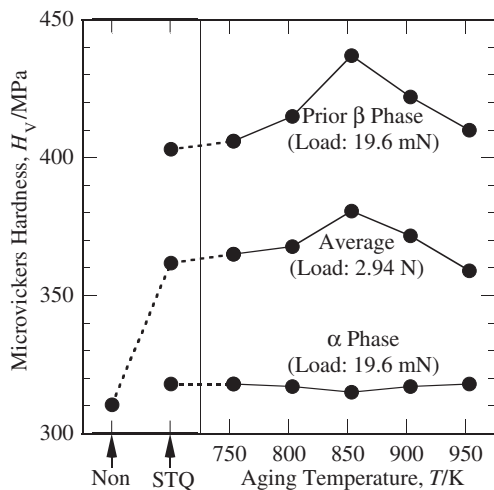


Fig. 5 Change in microvickers hardness of  $\alpha$  phase and prior  $\beta$  phase with the STQ treatment and subsequent aging for 40 s.

understood from the figure, the hardness of  $\alpha$  phase was almost unchanged for all the heat treatments. However, the hardness of prior  $\beta$  phase depended on the aging temperature

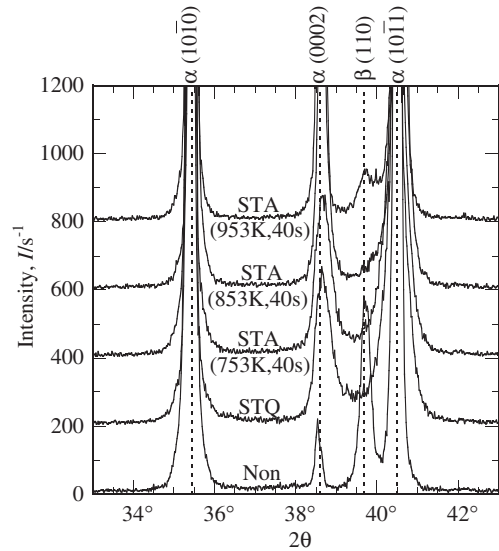


Fig. 6 X-ray diffraction profiles.

and its change closely corresponded with that in the average hardness. From this result, it is clear that the increase in the average hardness was due to the hardening of prior  $\beta$  phase.

### 3.2 X-ray diffraction, TEM observation and electron diffraction

Figure 6 shows the X-ray diffraction profiles of the non-treated, STQ-treated and STA-treated materials. Although the peak of  $\beta$  phase was seen on the non-treated material, it disappeared with the STQ treatment. Even after aging at 753 and 853 K for 40 s, no clear peak of  $\beta$  phase was detected. However, if the aging temperature was elevated to 953 K, the peak appeared again.

As Imam *et al.* pointed out,<sup>10)</sup> it is likely that the retained  $\beta$  phase cannot be differentiated from the  $\alpha'$  phase by X-ray diffraction measurements because the interplanar spacings in the two structures are nearly the same. Thereby, the only things surely proved from the obtained X-ray diffraction data are the absence of a stable  $\beta$  phase in the materials STQ-treated and aged at 753 and 853 K for 40 s, and its presence in the material aged at 953 K for 40 s.

According to Ref. 10), the retained  $\beta$  phase which is unconfirmed by X-ray diffraction measurement can be detected with the selected area electron diffraction technique. Using this technique, we also tried to confirm the presence of the retained  $\beta$  phase in the regions where TEM observations were conducted. The observed microstructures and obtained diffraction patterns are shown in Fig. 7. In this figure, the microstructure of the material aged at 853 K for a long time (Fig. 7(e)) is also shown for comparison.

From the features of the microstructure shown in Fig. 7(a), a relatively large amount of prior  $\beta$  phase seems to be transformed to acicular-shaped  $\alpha'$  phase by the STQ treatment. However, a part of the prior  $\beta$  phase was surely retained after this treatment because the diffraction pattern of  $\beta$  phase was obtained in the same region. The retained  $\beta$  phase may be located in the darkish area around the  $\alpha'$  phase in Fig. 7(a). In the material subsequently aged at 753 K (Fig. 7(b)), small acicular  $\alpha$  precipitations were found in the

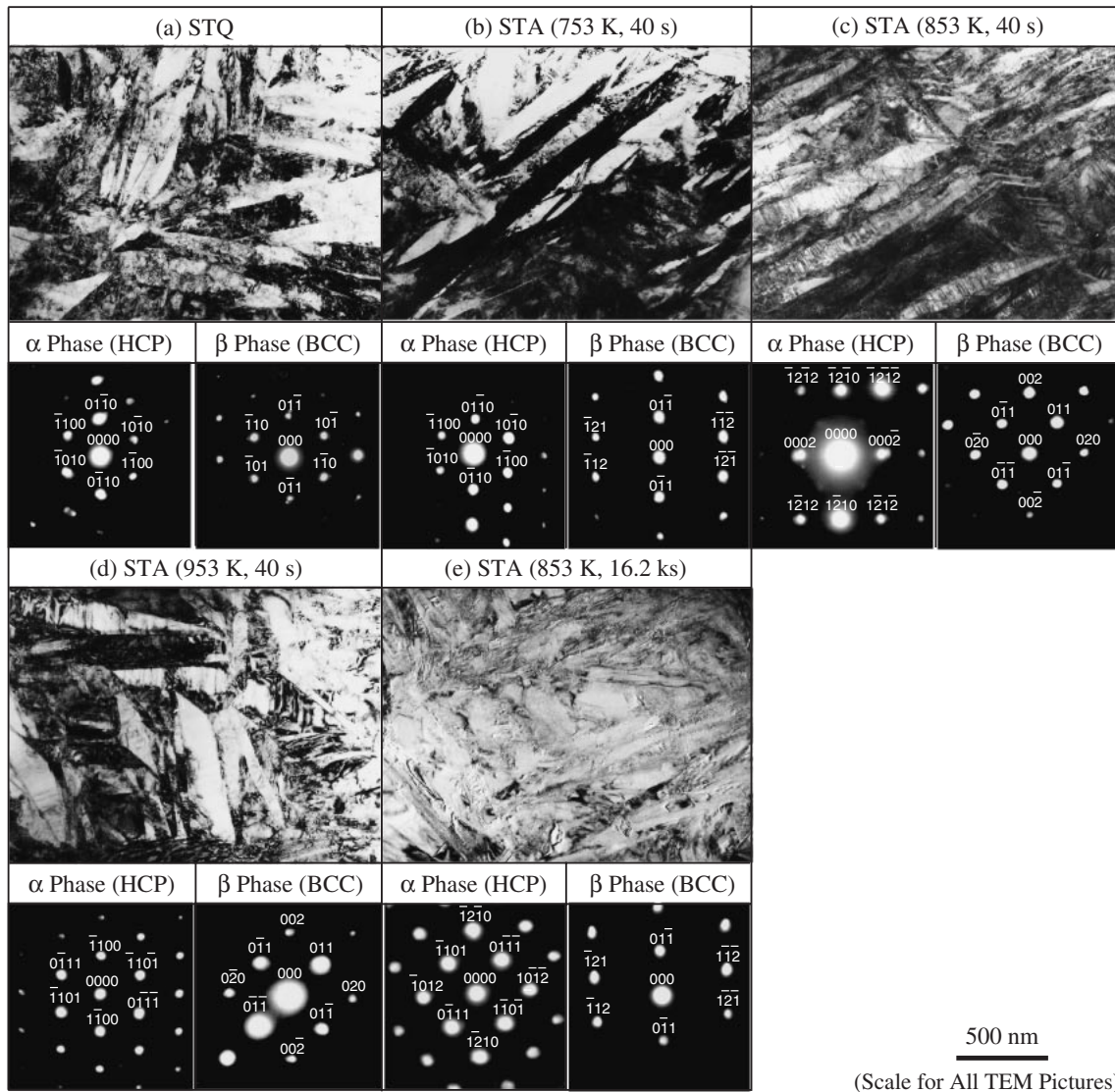


Fig. 7 Microstructures obtained by the TEM observations and the diffraction patterns detected in the same regions.

darkish region corresponding to the retained  $\beta$  phase. Upon elevating the aging temperature, it seems that the  $\alpha$  precipitations grew and the area occupied by  $\alpha$  precipitations increased (Figs. 7(b)–(d)).

The diffraction patterns of  $\beta$  phase were detected for all the aged materials. In the case of aging at 753 and 803 K, it is reasonable to think that these patterns show the existence of retained  $\beta$  phase since the X-ray diffraction data indicated no existence of stable  $\beta$  phase, as mentioned. However, when aging was performed at 953 K, the decomposition of  $\alpha'$  phase probably started and the diffraction pattern of  $\beta$  phase may have resulted from the stable  $\beta$  phase. That is because a clear peak of  $\beta$  phase was detected by the X-ray diffraction measurement and the feature at the right upper side of the figure (Fig. 7(d)) was similar to the microstructure of the material aged for a long time (Fig. 7(e)), where the acicular  $\alpha$  phase became rounder.

### 3.3 Mechanical properties

Figure 8(a) shows the effects of the STQ treatment and the subsequent aging on the mechanical properties of Ti-6Al-4V

alloy. Figure 8(b) gives the change in ratio between the yield strength and tensile strength,  $\sigma_{YS}/\sigma_{TS}$ , with the heat treatments. The true stress–strain curves of the tested materials and their features of fracture surfaces are shown in Figs. 9 and 10, respectively.

As may be understood from Fig. 8(a), while the yield strength and tensile strength were improved by the STQ treatment, the reduction of area also increased. With the subsequent aging, both strengths were further increased and the reduction of area was maintained above the value of the non-treated material. In the aged materials, the changes in strength clearly coincided with those in the average hardness (Fig. 5). The STA treatment including aging at 853 K for 40 s was suitable to improve the mechanical properties because the improvements of the yield strength and tensile strength were highest in all tested materials and no deterioration of ductility occurred.

It is thought that the above remarkable strengthening is mainly due to the refinement of prior  $\beta$  phase resulting from the formation of  $\alpha'$  phase and the precipitation of fine  $\alpha$  phase through the STQ treatment and aging (Fig. 7). However, we

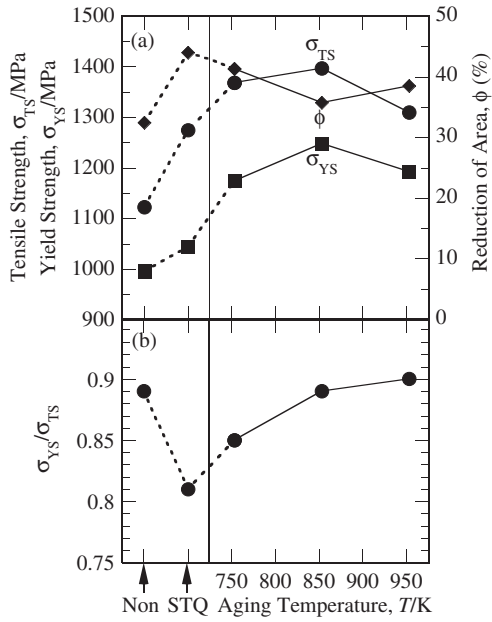


Fig. 8 (a) Change in the mechanical properties with the STQ treatment and subsequent aging for 40 s, (b) change in the ratio between the yield strength and tensile strength.

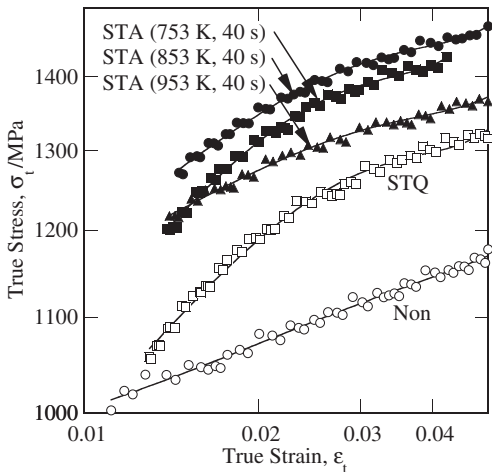


Fig. 9 True stress-strain curves ( $\log \epsilon_t - \log \sigma_t$  plots).

need to consider the behavior of retained  $\beta$  phase for explaining the high ductility of the heat-treated materials and their curved stress-strain relationships mentioned below.

In Fig. 9, although the stress-strain relationship of the non-treated material was linear, that of the STQ-treated material curved indicating that strong strain hardening occurred. When the material at the STQ condition was further aged, the degree of strain hardening decreased as the aging temperature increased. This tendency was reflected in the change in the ratio of  $\sigma_{YS}/\sigma_{TS}$  (Fig. 8(b)), namely, this ratio was lowest at the STQ condition and recovered with increasing aging temperature.

The above result can be related to the stress-induced martensite transformation of retained  $\beta$  phase. In the case of the STQ-treated material, it is reasonable to think that the curved stress-strain relationship and the resulting low ratio of  $\sigma_{YS}/\sigma_{TS}$  were caused by the stress-induced transformation of

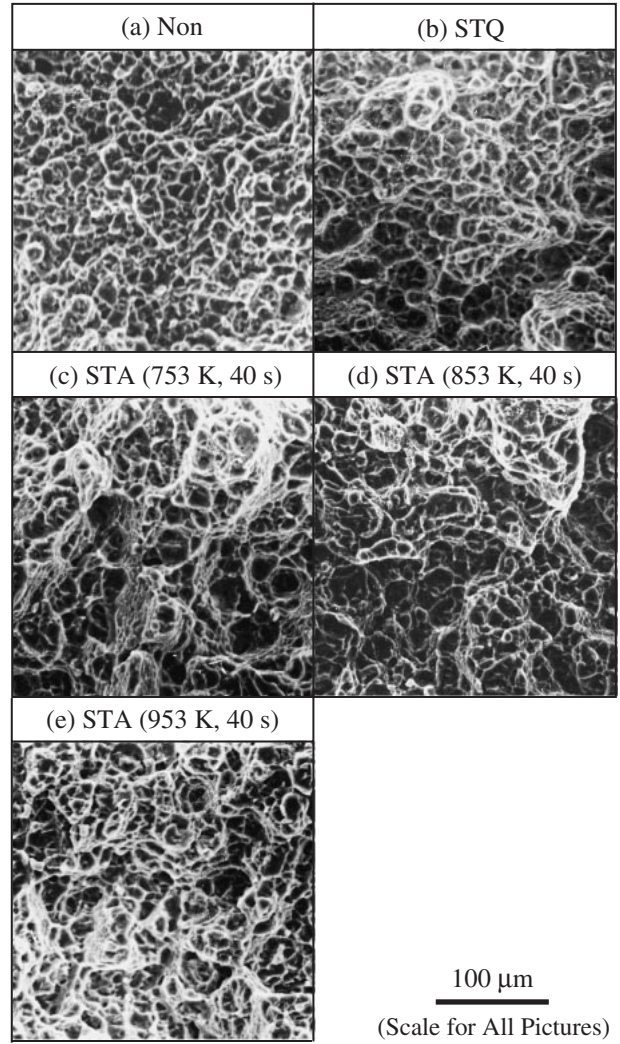


Fig. 10 Features of fracture surfaces.

retained  $\beta$  phase which started at a relatively lower applied stress level. For the aged materials, although no correct amount of retained  $\beta$  phase was obtained in this study, the features of the observed microstructures (Fig. 7) suggest that the amount of retained  $\beta$  phase decreased with elevation of the aging temperature. Based on this, we can give a rational explanation that the recovery in the ratio of  $\sigma_{TS}/\sigma_{YS}$  with the elevation of the aging temperature was due to the reduction in the amount of retained  $\beta$  phase.

The strengthening of metals usually accompanies a reduction in ductility. Actually, as we reported in the previous study,<sup>18)</sup> when Ti-6Al-4V alloy was STQ-treated at a higher temperature and was aged for a short time, the ductility deteriorated with a significant increases of the yield strength and tensile strength, and a number of facets were observed on the fracture surfaces. However, following the heat treatment conditions tested in this study, the ductility of the alloy was maintained at a level above that of the non-treated material and all the fracture surfaces of the heat-treated materials revealed ductile features (Fig. 10). From these results, it can be said that controlling the amount of retained  $\beta$  phase is an important factor in obtaining well-balanced microstructures of Ti-6Al-4V alloy.

#### 4. Conclusions

- (1) With the STQ treatment consisting of solution treatment at 1203 K for 60 s and water-quenching, the tensile strength of Ti–6Al–4V alloy was improved with an increase of ductility. However, the yield strength to tensile strength ratio was notably lower than that of the non-treated material. This probably resulted from the strain-induced transformation of retained  $\beta$  phase which occurred from a relatively low applied stress level.
- (2) Subsequent aging at 753–953 K for 40 s further improved both the yield strength and tensile strength of the STQ-treated material. It is thought that this improvement was caused by the precipitation of fine  $\alpha$  phase in retained  $\beta$  phase. In spite of the strengthening, the reduction of area was kept at a higher level than that of the non-treated material. This lack of deterioration of ductility may be because a sufficient amount of  $\beta$  phase to maintain the ductility was retained after the short-time aging.
- (3) The most appropriate heat treatment conducted in this study was the STA treatment consisting of STQ treatment at 1203 K for 60 s and aging at 853 K for 40 s. With this heat treatment, the yield strength and tensile strength were each increased by about 25% and the reduction of area was slightly increased, by about 9%.

#### Acknowledgements

This work was partially supported by the Ministry of Education, Culture, Sports, Science and Technology, Japan,

the Grant-in-Aid for Scientific Research (No. 16560069, 2004–2005). The authors gratefully acknowledge the support.

#### REFERENCES

- 1) G. Lutjering and J. C. Williams: *Titanium*, (Springer-Verlag, Berlin, 2003) p. 7.
- 2) R. G. Sherman and H. D. Kessler: *Trans. ASM* **48** (1956) 657–676.
- 3) B. L. Averbach, M. F. Comerford and M. B. Beve: *Trans. Metall. Soc. AIME* **215** (1959) 682–685.
- 4) J. C. Williams and M. J. Blackburn: *Trans. ASM* **60** (1967) 373–383.
- 5) P. J. Fopiano, M. B. Bever and B. L. Averbach: *Trans. ASM* **62** (1969) 324–332.
- 6) H. Sasano, S. Kmori, H. Kimura: *J. Jpn. Inst. Met.* **38-3** (1974) 199–205 (in Japanese).
- 7) *Metal Progress* **107-3** (1975) 72–73 (Data Sheet).
- 8) J. C. Chesnutt, C. G. Rhodes and J. C. Williams: *ASTM-STP* **600** (1976) 99–138.
- 9) J. R. Kennedy: *Mater. Sci. Eng.* **57** (1983) 197–204.
- 10) M. A. Imam and C. M. Gilmore: *Met. Trans. A* **14A** (1983) 233–240.
- 11) G. Sridhar, R. Gopalan and D. S. Sarma: *Metallography* **20** (1987) 291–310.
- 12) D. H. Kohn and P. Ducheyne: *J. Mater. Sci.* **26** (1991) 328–334.
- 13) H. Fujii: *Mater. Sci. Eng. A* **243** (1998) 103–108.
- 14) J. M. Manero, F. J. Gil and J. A. Planell: *Acta Mat.* **48** (2000) 3353–3359.
- 15) J. Nakahigashi and H. Yoshimura: *Trans. Met.* **43-11** (2002) 2768–2772.
- 16) J. I. Qazi, O. N. Senkov, J. Rahim and F. H. Froes: *Mater. Sci. Eng. A* **359** (2003) 137–149.
- 17) T. Morita, W. Niwayama, K. Kawasaki and Y. Misaka: *Trans. JSME (A)* **64-624** (1998) 2115–2120 (in Japanese).
- 18) T. Morita, Y. Misaka, K. Kawasaki, T. Iizuka: *J. Jpn. Inst. Met.* **68-10** (2004) 862–867 (in Japanese).